



HAL
open science

Continuous-time model identification of robot flexibilities for fast visual servoing

Luc Cuvillon, Edouard Laroche, Hugues Garnier, Jacques Gangloff, Michel de Mathelin

► **To cite this version:**

Luc Cuvillon, Edouard Laroche, Hugues Garnier, Jacques Gangloff, Michel de Mathelin. Continuous-time model identification of robot flexibilities for fast visual servoing. 14th IFAC Symposium on System Identification (SYSID'2006), Mar 2006, Newcastle, Australia. pp.1264-1269. hal-00109104

HAL Id: hal-00109104

<https://hal.science/hal-00109104>

Submitted on 23 Oct 2006

HAL is a multi-disciplinary open access archive for the deposit and dissemination of scientific research documents, whether they are published or not. The documents may come from teaching and research institutions in France or abroad, or from public or private research centers.

L'archive ouverte pluridisciplinaire **HAL**, est destinée au dépôt et à la diffusion de documents scientifiques de niveau recherche, publiés ou non, émanant des établissements d'enseignement et de recherche français ou étrangers, des laboratoires publics ou privés.

CONTINUOUS-TIME MODEL IDENTIFICATION OF ROBOT FLEXIBILITIES FOR FAST VISUAL SERVOING

Loïc Cuvillon* Edouard Laroche*
Hugues Garnier** Jacques Gangloff*
Michel de Mathelin*

* *Laboratoire des Sciences de l'Image de l'Informatique et
de la Télédétection (UMR CNRS 7005), Strasbourg 1
university, BP 10413, F-67412, Illkirch, France*

** *Centre de Recherche en Automatique de Nancy, CRAN
UMR 7039 CNRS-UHP-INPL, Université Henri Poincaré,
Nancy 1, BP 239, F-54506 Vandœuvre Cedex, France*

Abstract: This paper presents a general methodology for identifying the dynamical part of the continuous-time model of an articulated arm including flexibilities dedicated to visual servoing. Based on this model, a H_∞ control law is designed and implemented, allowing to reach high dynamics.

Keywords: System identification, continuous-time models, instrumental variable, visual servoing, robot arm, H_∞ control, flexible manipulator.

1. INTRODUCTION

This paper¹ presents the application results of a recently developed direct continuous-time model identification approach to identify a flexible robot arm for heart beating movement compensation. Generally, robotic arms are designed as rigid in order to be easily controllable. With the improvements in real-time computation and the development of control strategies allowing to efficiently handle flexibilities, it is not necessary anymore that the robots are rigid. This allows both to reduce their cost and to spare space. Moreover they become safer. This latter characteristic is certainly the most important for emerging application fields such as robotized surgery.

One emerging application in the medical domain is compensation of physiological movements in the context of robotic surgery (Ginhoux *et al.*, 2005). In this particular application, the robotic arm must be light for safety reasons and the band-

width must be high in order to follow properly the heart movements. Furthermore, the working configuration of the robot remains close to a nominal position that can be chosen in advance. Thus, it is not necessary that the model accounts for the nonlinearities due to a change of position. Most approaches available for flexible arm control rely on physical modeling. The traditional method consists in deriving the dynamical model thanks to the Euler-Lagrange equation with the assumed mode method (see de Luca and Siciliano (1991) for instance); the arm being torque controlled. The main drawback of these methods is that the model is hard to derive and can only be obtained with reasonable time for few degrees of freedom (DOF). Moreover, the parameters need to be estimated. Besides, robotic systems generally include torque and speed controllers implemented in the power drives whose transfer functions are unknown. For real-life applications, it is then crucial to be able to identify the dynamical model through experimental data.

System identification is an established field in the area of systems analysis and control. Although

¹ This report is related to the paper presented at the 14th IFAC Symposium on System Identification (SYSID'2006), Newcastle (Australia), pp. 1264-1269, March 2006.

dynamical systems in the physical world are normally formulated in the continuous-time (CT) domain, as differential equations, most system identification schemes have been based in the past on discrete-time (DT) models without concern for the merits of the more natural continuous-time models. Interest in CT approaches to system identification has however been growing in the last fifteen years. Furthermore, some recent publications have drawn attention to difficulties that can be encountered when utilizing DT estimation algorithms under conditions that are non-standard, such as rapidly sampled data and systems with widely different natural frequencies (Garnier *et al.*, 2003), (Ljung, 2003).

In this paper, we use a recently proposed identification method (Huselstein *et al.*, 2004) for multiple input single output (MISO) continuous-time linear systems described by multiple CT transfer functions with different denominators. This approach is based on the Simplified Refined Instrumental Variable for Continuous-time systems, denoted by SRIVC from hereon, which presents the advantage of yielding asymptotically efficient estimates in the presence of white measurement noise. Another interesting advantage of using this refined Instrumental Variable (IV) method is that a procedure based on the properties of the instrumental product matrix can be used for identifying the model structure prior to parameter estimation.

The main goal of this paper is therefore to present the application results of this recently proposed approach to identify a flexible robotic arm designed for heart-beating tracking. The considered methodology allows the model to include globally all the dynamics of the system, including the joint controllers. The obtained linear model is valid around a nominal position of the robot and can be recomputed easily as the camera is displaced. The general context of visual servoing and the structure of the model are presented in Section 2. The identification problem is then solved in Section 3. Finally, the model is used for designing a H_∞ controller and experimental results are presented in Section 4.

2. ROBOTIC SETUP

2.1 A setup dedicated to heart tracking

The setup considered is a prototype serial robot designed for heart beating movement compensation (see Figure 1). The arm has a light design in order to reach high dynamics. Therefore, small deflection may be expected during operation; the corresponding flexibilities must be accounted for in order to properly control the system.

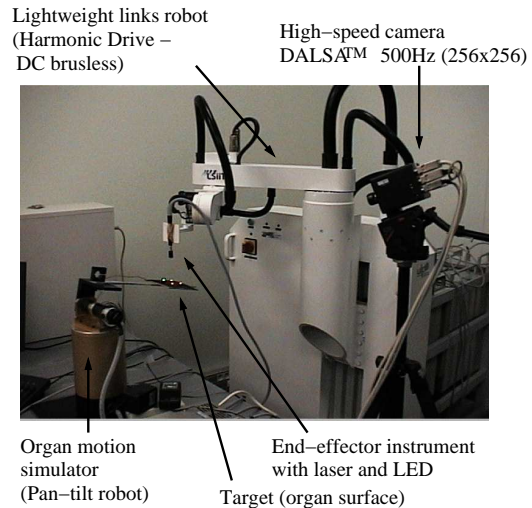


Fig. 1. Experimental setup

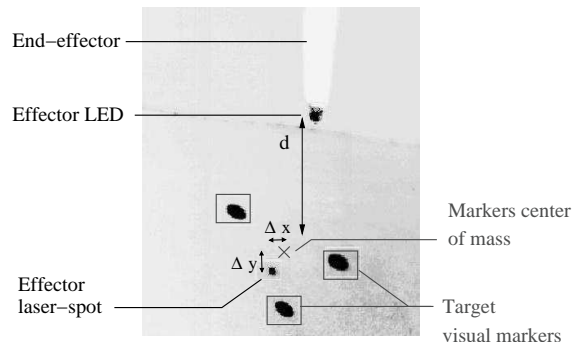


Fig. 2. Camera image of the visual task

A fixed high-speed camera (500 Hz) is used for evaluating the position of the instrument with respect to the organ and displacing it synchronously with the organ surface. Assuming that these features are placed at the surface of the organ and on the instrument, the task can be achieved by 2D visual servoing (Corke, 1996).

The chosen strategy uses some degrees of freedom for heart-movement compensation and preserves the others available for the surgeon. Three degrees of freedom being enough for positioning the instrument in front of a given point of the organ at a given distance, only the first 3 DOF need to be considered. The first DOF is prismatic and orthogonal with respect to the axes of the others DOF; their dynamics are then completely decoupled. In the paper is then considered the xy positioning of the tip of the instrument using the 2 first rotoid DOF. The instrument being equipped with a laser, the goal is to control the robot so that the projection of the laser follows the movements of the target within the highest bandwidth.

Before validating the approach on living animals, the system must be evaluated in laboratory. For this purpose, the organ is replaced by a simple 2-DOF arm (pan-tilt) that emulates the movements of the heart (organ motion simulator shown in

Figure 1). The image provided by the camera is shown in Figure 2. The two DOF considered in the paper are used to force the effector laser spot follow the center of mass of the three visual markers linked to the target *i.e.* $F = [\Delta x \ \Delta y]^T$ is controlled to zero.

2.2 Visual servoing

Let us consider the system composed of the robot, the camera and the target. The input signal u is composed of the speed references to the joint controllers. The outputs are the joint position vector q and vector F of coordinates of the features in the image. 2D visual servoing consists in controlling u so that F converges to a reference F^* .

The camera being either fixed with respect to the reference frame, either placed on the robot, F can be written as a function of q through the geometric model $F = F(\alpha)$, which is a static relationship, provided that the robot is rigid. Let us now consider the particular case where the joints are speed controlled and where the joint-speed dynamics can be neglected ($\dot{\alpha} = u$), a linearized model $\dot{F} = J(\alpha)u$ can be obtained where the interaction matrix $J(\alpha)$ is the Jacobian of $F(\alpha)$. The classical control strategy is therefore $u = kJ^\dagger(\alpha)(F^* - F)$ where J^\dagger denotes the pseudo-inverse of J . The system then exhibits first order behavior and the dynamics can be arbitrarily tuned by the scalar k , provided that the assumptions are true. If the working area is small enough, J^\dagger does not need to be reevaluated and can be estimated numerically by small displacements around the central position. Practically, the bandwidth is limited by the neglected dynamics.

2.3 Accounting for the dynamics

Several contributions have already been proposed in order to obtain high-speed visual servoing. Papanikolopoulos *et al.* took into account the effects of the latencies in the visual loop in a LQG control strategy (Papanikolopoulos *et al.*, 1993). Corke and Good used a linearized model of the visual loop involving delays but also the dynamics of the manipulator to tune PID controllers with a pole-placement technique (Corke and Good, 1996). More recently, it was proposed to account for the dynamics of the joint-speed control loop (Gangloff and de Mathelin, 2003). In this framework, the model can be written as:

$$\dot{F} = J(\alpha)\dot{\alpha} \quad (1)$$

$$\dot{\alpha} = H(s)u \quad (2)$$

where $H(s)$ contains the dynamics of the joint speed control loops; it is considered as a linear

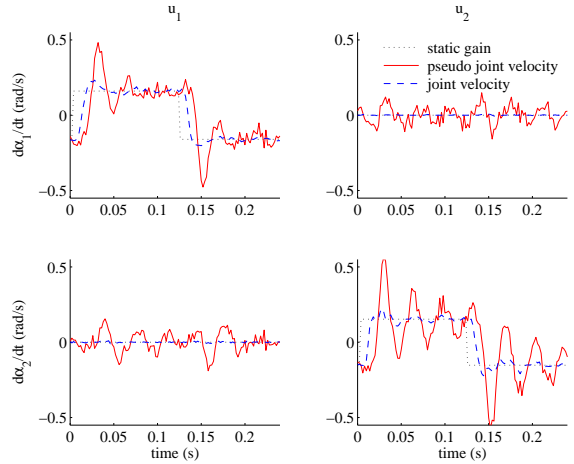


Fig. 3. Angular velocities and pseudo angular velocities step responses

time-invariant system to be identified from measurements of u and α . If the joint controllers are well tuned, the non-diagonal terms in $H(s)$ can be neglected and each single transfer function $H(s)$ can be independently estimated by using traditional SISO system identification methods. As the dynamic model is identified from measurements of u and α , it does not account for all the dynamics affecting the system such as segment deflexions.

More recently, this previous method was generalized. It was shown in (Cuvillon *et al.*, 2004) that the previous model (1,2) can account for all the dynamics provided that (i.) the DOF of the robot equals the DOF of the task and (ii.) $H(s)$ is identified from u and F ; $\dot{\alpha}$ being computed from $\dot{\alpha} = J^{-1}\dot{F}$. In this particular case, α does not correspond anymore to the joint position but includes fictitious displacements due to the deformations; let us call it *pseudo angular position*. The obtained model $H(s)$ is different from the one obtained with the previous method as soon as flexibilities are effective. This approach has already been used to design multivariable controllers (Cuvillon *et al.*, 2005). In this latter paper, each SISO model was identified independently leading to a final MIMO model of high order. The present paper focuses on the identification problem and shows how the use of a recent MISO identification method can help in obtaining a good controller. Notice that $H(s)$ is independent from the camera. In the case of a camera displacement, it is only necessary to estimate the corresponding interaction matrix J that can be done easily before operation.

In order to evaluate the difference between the two models previously mentioned, the step responses of the angular velocities and pseudo-angular velocities are given in Figure 3. The four curves represent the angular velocities of the two joints for step excitation respectively on u_1 (left hand side) and u_2 (right hand side). The angular veloci-

ties are computed by differentiation of the angular positions α_1, α_2 sampled at 500 Hz. The pseudo-angular velocities are computed via $\dot{\alpha} = J^{-1}\dot{F}$; \dot{F} being computed by differentiation and J being estimated from small displacements. One can notice that the responses of the actual angular velocities (in dashed) are well damped and decoupled whereas the pseudo-angular velocities (in plain), estimated from the feature velocities in the image are not well damped and not so well decoupled. The challenge presented in the paper consists in identifying a linear model corresponding to the pseudo-angular velocities.

3. CT MODEL IDENTIFICATION OF THE ROBOT FLEXIBILITIES

In this section, the application results of one particularly successful and recently developed stochastic identification method (Huselstein *et al.*, 2004) are presented. This IV type of approach not only ensures that the estimate converges to statistically optimum values in the case of additive white noise, it also generates information on the parametric error covariance matrix which can be used in an associated procedure to identify the orders of the component transfer function models. The proposed estimation scheme is available in the CONTSID² toolbox.

The recently proposed version of the optimal SRIVC method for multiple input single output systems where the characteristic polynomials of the CT transfer functions associated with each input are not constrained to be identical (Huselstein *et al.*, 2004) is used here to estimate all transfer functions $G_{ij}(s)$ defined in:

$$\begin{pmatrix} \dot{\alpha}_1(s) \\ \dot{\alpha}_2(s) \end{pmatrix} = \begin{pmatrix} G_{11}(s) & G_{12}(s) \\ G_{21}(s) & G_{22}(s) \end{pmatrix} \begin{pmatrix} u_1(s) \\ u_2(s) \end{pmatrix} \quad (3)$$

with :

$$G_{ij}(s) = \frac{B_{ij}(s)}{F_{ij}(s)} = \frac{\sum_{k=0}^{m_{ij}} b_k s^k}{\sum_{k=0}^{n_{ij}} f_k s^k} \quad f_{n_{ij}} = 1. \quad (4)$$

3.1 Experiment design

Excitation signals are defined in order to sensitive at best the bandwidth of the process while respecting the working constraints. The inputs are therefore chosen as uncorrelated Pseudo Random Binary Signals (PRBS) of maximum length with suitable magnitude to stay around the operating point for estimating a linear model. Portions of experimental input-output signals are displayed in Figure 4. The sampling time is set to 2 ms. Each experiment lasts around 10 s. Several data sets

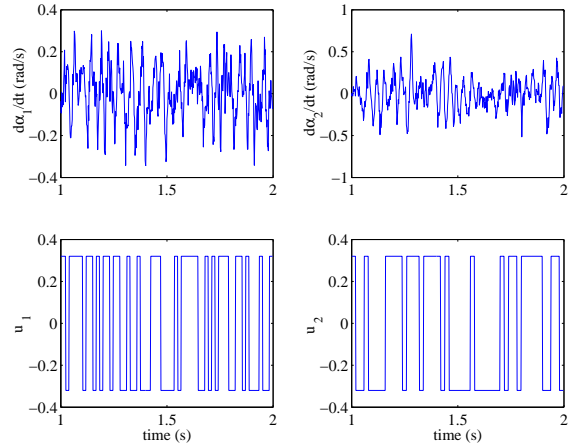


Fig. 4. Portion of the raw input-output data used for model identification

corresponding to different PRBS are collected. One of the data sets is used for model order selection and parameter estimation while the other data set are reserved for model validation only.

3.2 Model order selection

The model order selection procedure presented in (Huselstein *et al.*, 2004) is used to determine the transfer function orders of the flexible robot arm model. For each output, a large number of models are estimated for a wide range of model orders. The best 10 model structures for each output are given in Table 1. Here, the first two columns specify the numerator orders for each transfer function; the third and fourth column report the denominator orders and the fifth and sixth column are both model order selection criteria: YIC (Young's Information criteria, see *e.g.* Young (2002)) and R_T^2 is the well-known coefficient of determination based on the simulation error, defined as

$$R_T^2 = 1 - \frac{\hat{\sigma}_\varepsilon^2}{\hat{\sigma}_y^2}, \quad (5)$$

where $\hat{\sigma}_y^2$, $\hat{\sigma}_\varepsilon^2$ denote respectively the variance of the measured output and the variance of the simulation error. R_T^2 is a measure of how well the model output explains to the system output and will be close to 1 in low noise situations. However, R_T^2 tends to overestimate the model orders. The Young's Information Criterion (YIC) is more complex and provides a measure of how well the parameters are defined statistically: the more negative the YIC, the better the definition. However it may lead to underestimate the model orders. Both criteria are inspected to find the orders for which R_T^2 is sufficiently high to indicate a good explanation of the data and the YIC is sufficiently negative to indicate well defined parameter estimates. Model structures that respect

² see <http://www.cran.uhp-nancy.fr/contsid/>

Output 1, α_1					
m_{11}	m_{12}	n_{11}	n_{12}	YIC	R_T^2
1	1	5	2	-8.033	0.721
1	2	5	2	-8.033	0.721
3	1	4	2	-7.624	0.727
4	1	4	2	-7.624	0.727
3	2	4	2	-7.624	0.727
4	2	4	2	-7.624	0.727
3	1	4	4	-7.473*	0.772
4	1	4	4	-7.473	0.772
1	1	2	2	-7.200	0.691
2	1	2	2	-7.200	0.691

Output 2, α_2					
m_{21}	m_{22}	n_{21}	n_{22}	YIC	R_T^2
1	1	4	2	-9.609	0.833
1	2	4	2	-9.609	0.833
1	3	4	4	-9.267*	0.870
1	4	4	4	-9.267	0.870
1	2	4	4	-9.237	0.862
2	3	4	4	-7.081	0.882
2	4	4	4	-7.081	0.882
2	2	4	4	-7.063	0.874
1	1	4	5	-6.905	0.873
1	2	4	5	-6.670	0.879

Table 1. Best 10 model structures according to YIC and R_T^2

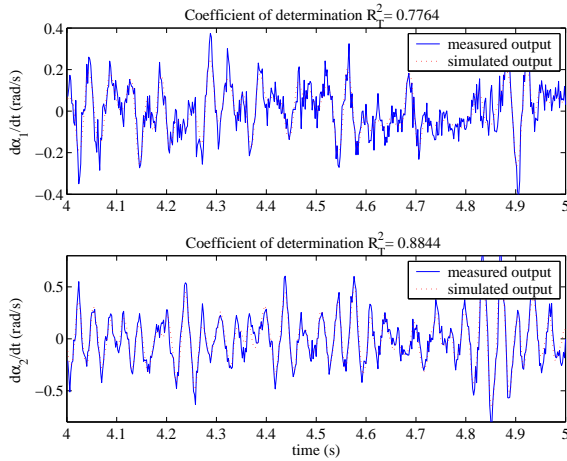


Fig. 5. Cross-validation results

the above condition have finally been selected and are referenced by ‘*’ in Table 1.

3.3 Cross-validation results

To evaluate the quality of the estimated transfer function models, a cross-validation procedure has been applied to data that were not used to build the model. Cross-validation results are plotted in Figure 5, where it may be observed that there is a satisfactory reproduction of the two output behavior by the transfer function matrix model.

The CT model identification approach exploited here provides a reduced-order differential equation model with stochastically defined parameters (the parameter estimates and their associated covariance matrix) that can be used for process simula-

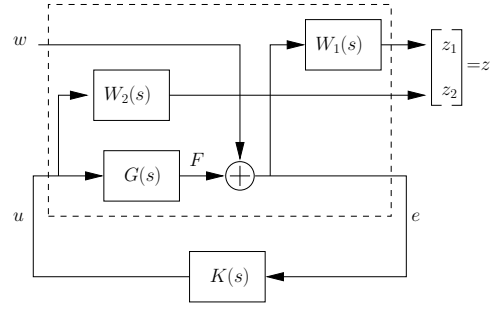


Fig. 6. Generalized plant with weighting function diagram

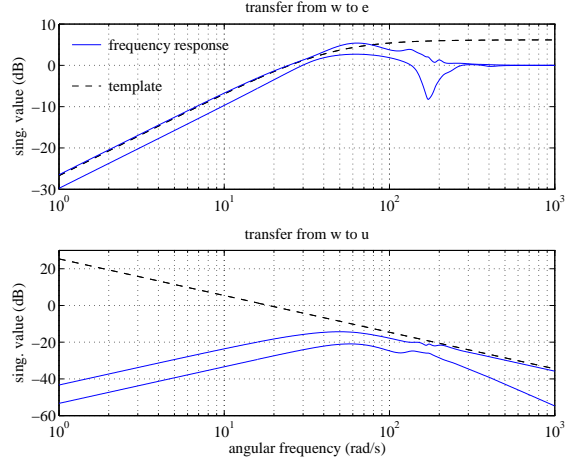


Fig. 7. Closed-loop transfer functions

tion purpose or can be the basis for control system design as presented in the next section.

4. H_∞ CONTROL

Based on the synthesis scheme presented in Figure 6 where the control scheme is augmented of weighting functions $W_1(s)$ and $W_2(s)$, the Glover-Doyle algorithm (Doyle *et al.*, 1989) enables to design a controller $K(s)$ allowing to stabilize the system and minimize H_∞ norm of transfer T_{zw} from w to z . The weighting functions are tuned in order to shape the closed-loop transfer functions. Indeed, $\bar{\sigma}(W_1^{-1}(j\omega))$ and $\bar{\sigma}(W_2^{-1}(j\omega))$ are templates for respectively $\bar{\sigma}(T_{ew}(j\omega))$ and $\bar{\sigma}(T_{uw}(j\omega))$ in the frequency domain. Good tracking properties are conferred by lowering $\bar{\sigma}(T_{ew}(j\omega))$ in low frequencies; robustness is conferred by lowering $\bar{\sigma}(T_{uw}(j\omega))$ in high frequencies (roll-off effect). Design is done in the CT domain based on the identified CT-model. Frequency responses and templates corresponding to the chosen weighting functions are shown in Figure 7. The obtained bandwidth (20 rad/s) is enough for tracking heart beating effectively.

The DT controller for implementation is obtained using the Tustin bilinear transform. Simulation and experimental results in response to step per-

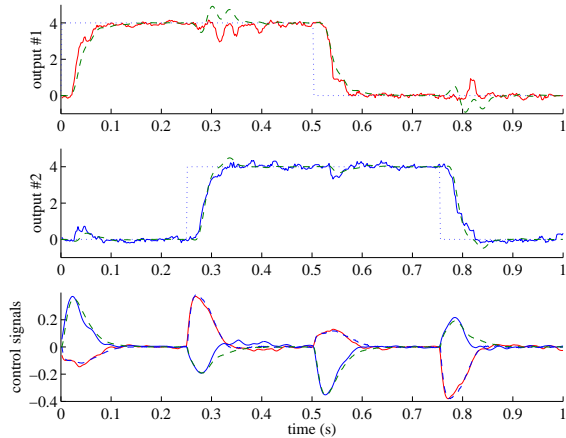


Fig. 8. Time-domain experiment and simulation
turbations are given in Figure 8. The perturbation signal is followed properly with good decoupling between the two axis. Moreover, the model and the experimental setup exhibit very close behavior.

5. CONCLUSION

This paper has presented the application results of a recently developed direct continuous-time model identification approach to identify a flexible robot arm for heart beating movement compensation. The direct continuous-time approach has been chosen here since it offer advantages over alternative discrete-time model identification methods when applied to systems such as the flexible robot arm, with widely separated modes and rapidly sampled data. Moreover, the chosen identification procedure directly provides a continuous-time transfer function model which has been used to design a H_∞ controller directly in the continuous-time domain. Based on the identified model, the designed control could effectively handle the robot flexibilities.

ACKNOWLEDGMENT

This work is supported by a “Bourse de Docteur Ingenieur” grant from the Alsace Regional Council and the Centre National de la Recherche Scientifique.

REFERENCES

- Corke, P. I. and M. C. Good (1996). Dynamic effects in visual closed-loop systems. *IEEE Transactions on Robotics and Automation* **12**(5), 671–683.
- Corke, Peter I. (1996). *Visual control of robots*. Research Studies Press Ltd.. Taunton, Somerset, U.K.
- Cuvillon, L., E. Laroche, J. Gangloff and M. de Mathelin (2005). GPC versus H_∞ control for fast visual servoing of a medical manipulator including flexibilities. In: *International Conference on Robotics and Automation*. Barcelona-Spain.
- Cuvillon, L., J. Gangloff, E. Laroche, R. Ginhoux and M. de Mathelin (2004). Flexible modes identification of a surgical robot using 500 hz imaging for high-speed visual servoing. In: *Proceedings of Mechatronics and Robotics 2004*.
- de Luca, A. and B. Siciliano (1991). Closed-form dynamic model of planar multilink lightweight robots. *IEEE trans. on Syst., Man and Cybernetics* **21**(4), 826–839.
- Doyle, J.C., k. Glover, P.P. Khargonekar and B.A. Francis (1989). State-space solutions to standard H_2 and H_∞ control problems. *IEEE Transactions on Automatic Control* **34**(8), 831–847.
- Gangloff, J. A. and M. F. de Mathelin (2003). High speed visual servoing of a 6 DOF manipulator using multivariable predictive control. *Advanced Robotics* **17**(10), 993–1021. Special issue : advanced 3D vision and its application to robotics.
- Garnier, H., M. Mensler and A. Richard (2003). Continuous-time model identification from sampled data. Implementation issues and performance evaluation. *International Journal of Control* **76**(13), 1337–1357.
- Ginhoux, R., J. Gangloff, M. de Mathelin, L. Soler, M. Arenas Sanchez and J. Marescaux (2005). Active filtering of physiological motion in robotized surgery using predictive control. *IEEE Transactions on Robotics* **21**(1), 67–79.
- Huselstein, E., M. Gilson, H. Garnier and A. Richard (2004). Instrumental variable algorithms for multiple input systems described by multiple continuous-time TF models. In: *Asian Control Conference*. Melbourne (Australia).
- Ljung, L. (2003). Initialisation aspects for subspace and output-error identification methods. In: *European Control Conference (ECC’2003)*. Cambridge (U.K.).
- Papanikolopoulos, N.P., P.K. Khosla and T. Kanade (1993). Visual tracking of a moving target by a camera mounted on a robot: combination of control and vision. *IEEE Transactions on Robotics and Automation* **9**(1), 14–35.
- Young, P.C. (2002). Comments on “On the estimation of continuous-time transfer function”. *International Journal of Control* **75**(9), 693–697.